

Universal scaling property in bifurcation structure of Duffing's and of generalized Duffing's equations

Shin-ichi Sato, Masaki Sano, and Yasuji Sawada

Research Institute of Electrical Communication, Tohoku University, Sendai 980, Japan

(Received 2 May 1983)

Computer calculation for the numerical solution of Duffing's and generalized Duffing's equations shows global scaling properties for the bifurcation in parameter space. These scaling properties are discussed in terms of a one-dimensional map. The analysis based on a piecewise linear approximation gave results in good agreement with the experimentally observed scaling behavior.

I. INTRODUCTION

In recent years, many studies have been done on new universal behavior in chaotic dynamical systems. Period doubling, intermittent transition to chaos, and other related phenomena were investigated in detail by many authors from the viewpoint of scaling properties. They are all related to local bifurcation structure which occurs prior to chaos by changing parameters continuously.¹⁻³ However, a large number of phenomena observed in physical systems, chemical reactions, and biological systems exhibit interesting global bifurcation structure as well as the local bifurcations in parameter space. These global structures correspond to repeating transitions from a phase-locking state to another phase-locking state or to a chaotic state and vice versa.⁴ Only a few authors have discussed the global aspects of these bifurcation sets. Among these authors Tomita and Tsuda explained a global bifurcation structure in the Lorentz system by using one-dimensional mapping.⁵ They have also succeeded in interpreting and predicting the experimental results for a Belousov-Zhabotinsky reaction in a stirred-flow reactor utilizing similar methodology.⁶

A simplest example presenting a global bifurcation structure is forced nonlinear oscillators which are widely observed in physical,⁷⁻⁹ chemical, and biological systems. However, scaling properties among these phase-locking regions and chaotic regions have not been noticed until recently.

Recently Kaneko presented similarity and scaling properties of each periodic state in connection with a map of a circle.¹⁰ Almost simultaneously, Sano and Sawada reported a scaling behavior of the bifurcation parameters in a differential system of coupled chemical reaction systems.¹¹ In this paper we consider Duffing's equation, which represents nonlinear oscillation in an X^4 potential with external periodic force and damping, or generalized Duffing's equation, an oscillation in an X^{2n} potential. As regards Duffing's equation, Ueda has extensively investigated chaotic phenomena mainly concerning the appearance of the homoclinic orbit.¹²⁻¹⁴ The system can be a good prototype for studying chaotic phenomena in ordinary differential equations because it presents various types of transitions, e.g., period-doubling bifurcation, sub-

critical transition to chaos, and homoclinicity. Concerning the structure of global bifurcation sets, Kawakami and Matsuo¹⁵ have pointed out that similarity can be observed in bifurcation sets of Duffing's equation by computer experiment.

The purpose of the present work is to show for the first time the existence and interpretation of scaling properties in global bifurcation sets which can appear in a wide class of forced nonlinear oscillations. We confirmed numerically the similarity and scaling property of global bifurcation sets in Duffing's equation and even in generalized Duffing's equations.

II. EXPERIMENTAL RESULTS

Duffing's equation with cubic nonlinearity is

$$\frac{d^2x}{dt^2} + k \frac{dx}{dt} + x^3 = B \cos t, \quad (1)$$

where k is the damping rate and B is the modulation amplitude. Equation (1) can be rewritten as simultaneous equations,

$$\frac{dx}{dt} = y, \quad (2a)$$

$$\frac{dy}{dt} = -ky - x^2 + B \cos t. \quad (2b)$$

This system has a symmetry under the transformation S ,

$$S: (x, y, t) \rightarrow (-x, -y, t + \pi).$$

Therefore, if ψ is a solution of Eq. (2), then $S\psi$ is also a solution. In order to characterize the bifurcation diagram by topological properties of solution, we introduce the notation P_s , P_a , and X . Periodic and chaotic orbits are denoted by $P_a^\pm(n, m)$, $P_s(m, n)$, and X , where by $P(n, m)$ we mean a periodic orbit which cuts the $y=0$ plane from the positive to negative y direction at n different values of x and cuts the $y=0$ plane in the opposite direction at m different values of x . The indices s and a indicate symmetric and antisymmetric solution, and the \pm represents pair solutions connected by the transformation S .

A coarse bifurcation process with increasing B is com-

posed of the alternative appearance of periodic and chaotic states:

$$\cdots \rightarrow P \rightarrow X \rightarrow P \rightarrow X \rightarrow \cdots$$

The chaotic region would appear between two periodic states which have topological properties different from each other. When k is small the bifurcation process can be described, in more detail, as

$$\cdots \rightarrow P_s(n,n) \rightarrow \left\{ \begin{matrix} P_a^+(n,n) \\ P_a^-(n,n) \end{matrix} \right\} \xrightarrow{I} X \xrightarrow{D} \left\{ \begin{matrix} P_a(n,n+1) \\ P_a(n+1,n) \end{matrix} \right\} \xrightarrow{I} X \xrightarrow{D} P_s(n+1,n+1) \rightarrow \cdots$$

(double bifurcation process), where the curly brackets mean coexistence of symmetric pair solutions. The route to chaos is period doubling (indicated by I) or subcritical transition (indicated by D). On the other hand, when k is relatively large the bifurcation process is

$$\cdots \rightarrow \left\{ \begin{matrix} P_a(n,n+1) \\ P_a(n+1,n) \end{matrix} \right\} \xrightarrow{I} X \xrightarrow{D} P_s(n+1,n+1) \xrightarrow{D} \left\{ \begin{matrix} P_a(n+1,n+2) \\ P_a(n+2,n+1) \end{matrix} \right\} \rightarrow \cdots$$

(single bifurcation process). Figure 1 shows some examples of the periodic orbits and Fig. 2 shows an example of transition from the periodic state to the chaotic state. In the chaotic region the fine structure of windows of phase-locking states is inevitably observed in addition to the homoclinic orbits observed by Ueda.¹⁴

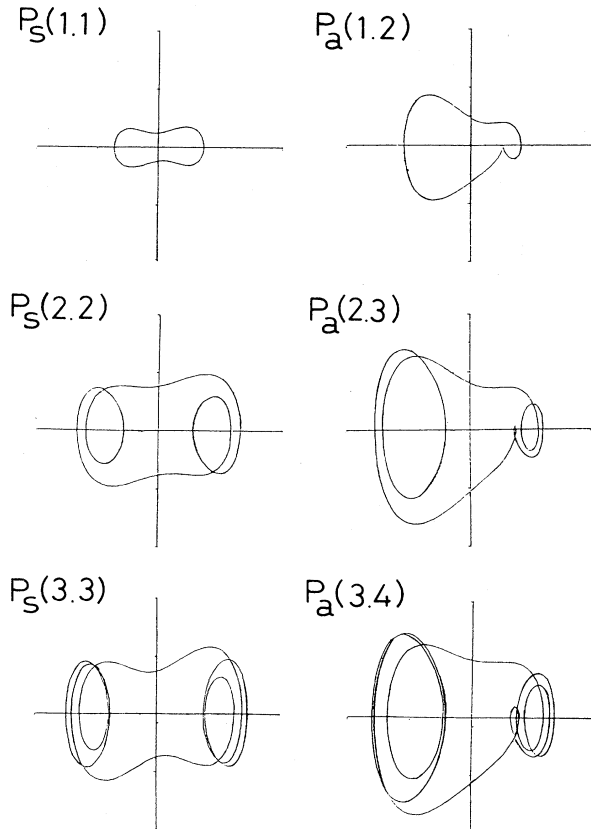


FIG. 1. Periodic orbits of Duffing's equation in phase-locking regions at $k=0.3$. $P(1,1)$ for $B=2.0$, $P(1,2)$ for $B=5.0$, $P(2,2)$ for $B=15.0$, $P(2,3)$ for $B=31.0$, $P(3,3)$ for $B=70.0$, $P(3,4)$ for $B=92.0$.

Present computer experiments have elucidated a series of similar bifurcation structures in k - B parameter space as shown in Fig. 3. A part of this structure in the small- B region was studied before¹⁵ but the region with a large value of B has not been investigated. To examine quantitatively the scaling properties for the bifurcation process, we measured B_m as shown by Fig. 3. B_m represents the initiation value of B for a period-doubling bifurcation from a periodic state $P_a(n,n+1)$ where $m=2n+1$. The logarithmic plot of B_m vs m shown in Fig. 4 exhibits a relation

$$B_m \propto m^\alpha, \tag{3}$$

where $\alpha=3.18$ for the ordinary Duffing's equation.

Similar experiments were carried out for the generalized Duffing's system

$$\frac{d^2x}{dt^2} + k \frac{dx}{dt} + x^{2\nu+1} = B \cos t, \tag{4}$$

where $\nu=2,3,4,\dots$. The numerical results for these bifurcation sets are shown in Fig. 4. We have obtained $\alpha=2.57$ for $\nu=2$, $\alpha=2.42$ for $\nu=3$.

In order to understand the scaling behavior of the bifurcation sets we take here a Poincaré mapping obtained from "the maximum absolute point" of x . Let $p=(t,x,y)$ be a solution of Eq. (2). The maximum absolute point is $p(t,x,0)$ in $x>0$ (but $d^2x/dt^2<0$) and in $x<0$ (but $d^2x/dt^2>0$). If we let $p_n=(t_n,x_n,0)$, $p_{n+1}=(t_{n+1},x_{n+1},0)$ be two successive maximum absolute points, then one obtains a discrete dynamical system,

$$T: p_n \rightarrow p_{n+1}. \tag{5}$$

Near the bifurcation point from a periodic to a chaotic state the point sequence given by Eq. (5) was found by computer experiments to move on invariant sets which can be approximately regarded as one-dimensional attractors embedded in the x - t plane. Therefore, one can reduce the map given by Eq. (5) to the following one-dimensional map which is useful in order to discuss the topological structure of Duffing's system:

$$f: \theta_n \rightarrow \theta_{n+1}, \tag{6}$$

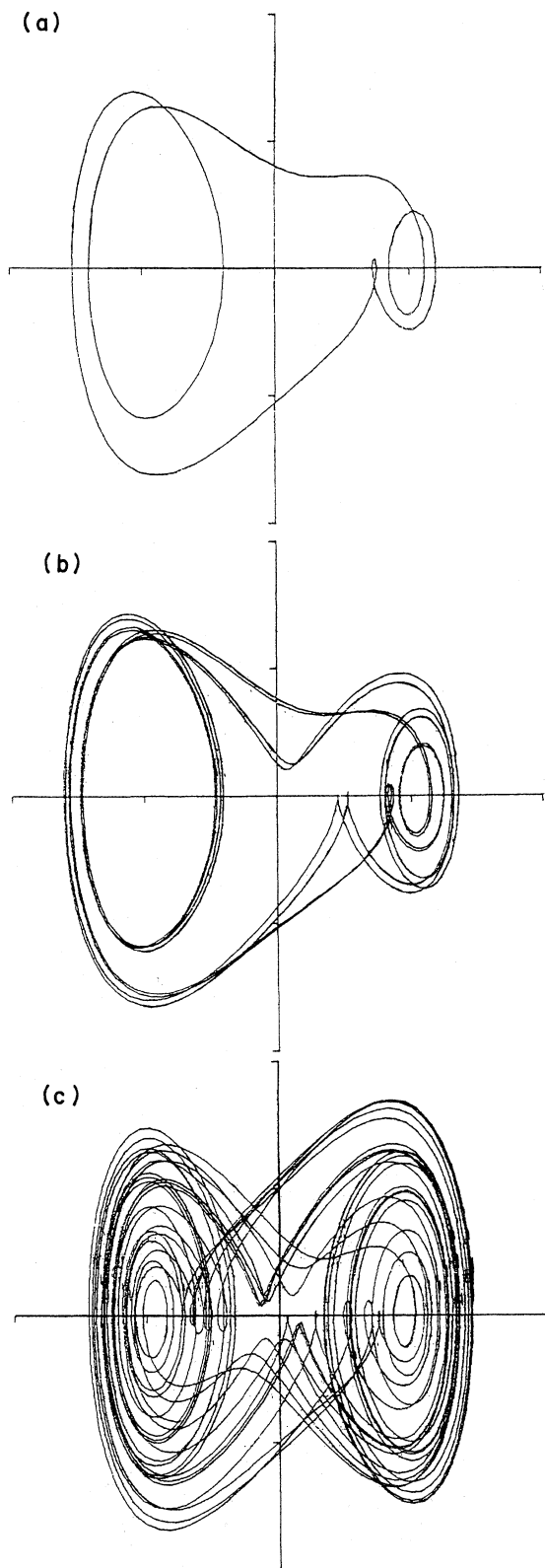


FIG. 2. Transition from a periodic state to chaotic state at $k=0.3$ for (a) $B=31.0$, (b) $B=36.0$, (c) $B=40.0$. System in a phase-locking state displays period-doubling bifurcations and leads to chaos.

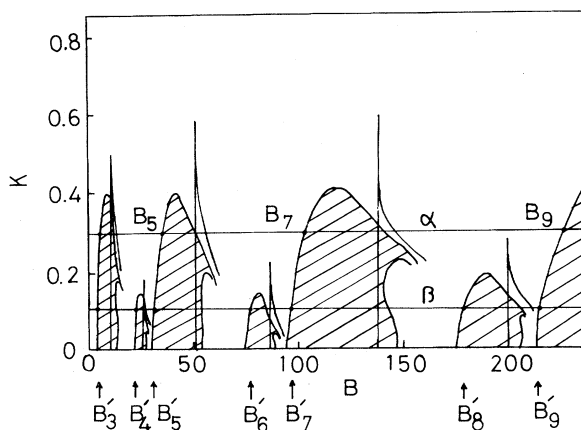


FIG. 3. Phase diagram in k - B parameter space. Parts of the hatched line are the regions where the period of the limit cycle is not 2π , i.e., period-doubling bifurcations, chaotic, and window regions. There exist hysteresis phenomena on a cusp line. Similar bifurcation sets have a scaling law vs the parameter B . Lines α and β are examples of "single bifurcation process" and "double bifurcation process," respectively. B_m and B'_m are the critical values of period-doubling bifurcation.

where $\theta_n = t_n/2\pi$. Figures 5(a) and 5(b) demonstrate the map f for two different values of B . The obtained map can be regarded as

$$f(\theta_n) = \theta_n + \Omega(k, B) + N(\theta_n, K, B), \quad (7)$$

where Ω is a constant independent of θ_n and the magni-

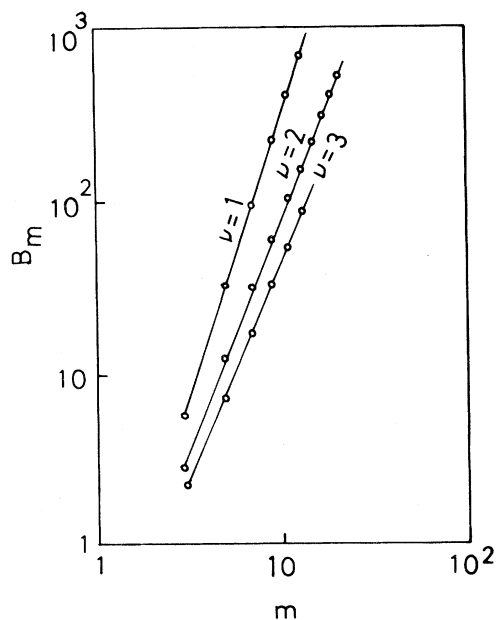


FIG. 4. Scaling law in the generalized Duffing's system. Scaling law obtained by Eq. (4) where $\alpha=3.18$ for $\nu=1$, $\alpha=2.57$ for $\nu=2$, $\alpha=2.24$ for $\nu=3$.

tude was experimentally found to be proportional to $B^{-1/3}$. Ω has a very weak dependence of k . $N(\theta_n, k, B)$ is a nonlinear contribution in the map which is responsible for the occurrence of chaos.

III. DISCUSSION

In this section we discuss the reason for the scaling law obtained in the preceding section. The map f represented by Eq. (7) reminds us of the map which has been studied by Shenker,¹⁶ but f has a global structure shown by Eq. (3) which is different from the map by Shenker.

At first let us consider the two-dimensional map T for the generalized Duffing's equation and introduce the piecewise linearized version at the small interval $t_n \leq t < t_{n+1}$ where $P_n = (t_n, x_n, 0)$, the maximum absolute point. Thus

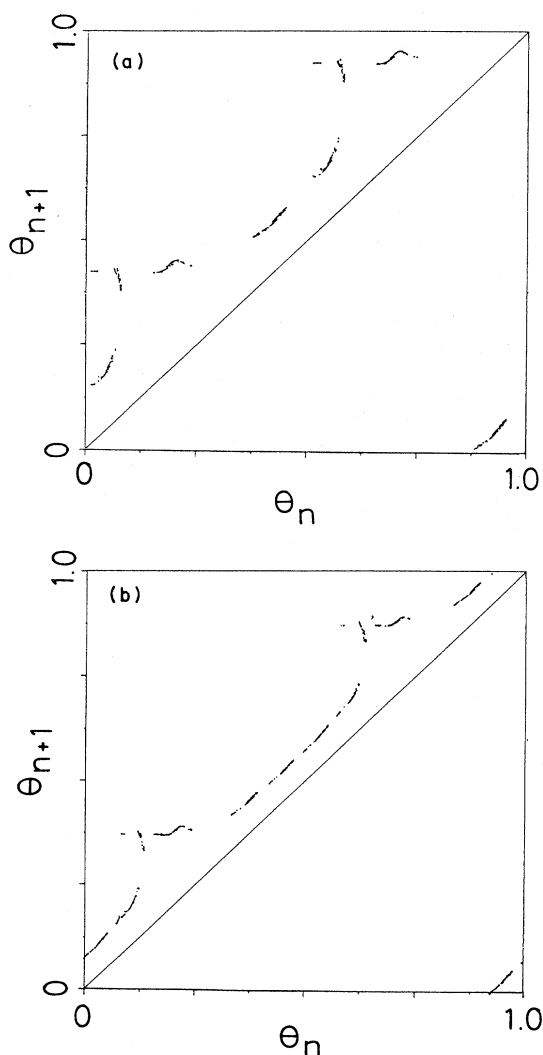


FIG. 5. One-dimensional map obtained by computer simulations. (a) $k=0.3$, $B=130.0$; (b) $k=0.3$, $B=500.0$. Map is expressed as $\theta_{n+1} = \theta_n + \Omega + N(\theta_n)$ where $\Omega \cong 0.15$ and $N(\theta_n)$ is the nonlinear contribution.

$$\frac{d^2x}{dt^2} + k \frac{dx}{dt} + a(x_n)x = B \cos t, \quad (8)$$

where $a(x_n) = (2\nu + 1)x^{2\nu}$. In the real Duffing's system the motion of a forced pendulum is very complicated but Eq. (8) is valid when the interval $[t_n, t_{n+1}]$ is sufficiently small (i.e., B is sufficiently large) and x_n is large. When $a(x_n) > k^2/4$, the solution of the piecewise linear equation is

$$x(t) = A \exp\left[-\frac{k}{2}t\right] \cos(\omega_n t + \delta_1) + \frac{B}{[(a-1)^2 + k^2]^{1/2}} \cos(t + \delta_2), \quad (9)$$

where A, δ_1 are determined by initial conditions, $\delta_2 = \tan^{-1}[k/(a-1)]$, $\omega_n = [a(x_n) - k^2/4]^{1/2}$. From the definition of map T , initial conditions are $x(t_n) = x_n$, $dx(t_n)/dt = 0$ and

$$\theta_{n+1} \approx \theta_n + \frac{1}{\omega_n}, \quad (10a)$$

$$x_{n+1} \approx x \left[2\pi\theta_n + \frac{2\pi}{\omega_n} \right], \quad (10b)$$

where $\theta_n = t_n/2\pi \pmod{1}$. θ_n is the phase of the periodic perturbation. When $k \ll 1$, $B \gg 1$, and $x_n \gg 1$, then Eq. (10) is

$$\theta_{n+1} \approx \theta_n + \frac{1}{(2\nu+1)^{1/2} |x_n|^\nu}, \quad (11a)$$

$$x_{n+1} \approx x_n - \frac{2\pi B}{(2\nu+1)^{3/2} |x_n|^{3\nu}} \sin 2\pi\theta_n. \quad (11b)$$

We approximate the recursion relation Eq. (11) by a differential equation on which the step space is $d\tau$,

$$\frac{d\theta}{d\tau} \approx \frac{1}{(2\nu+1)^{1/2} |x|^\nu}, \quad (12a)$$

$$\frac{dx}{d\tau} \approx \frac{2\pi B}{(2\nu+1)^{3/2} |x|^{3\nu}} \sin 2\pi\theta. \quad (12b)$$

These equations are readily integrated;

$$x \approx (B \cos 2\pi\theta)^{1/(2\nu+1)}. \quad (13)$$

This result was found to be in good agreement with computer simulations near bifurcation points. The map f defined by Eq. (6) is

$$\theta_{n+1} = f(\theta_n) \approx \theta_n + (2\nu+1)^{-1/2} (|B \cos 2\pi\theta_n|)^{-\nu/(2\nu+1)}. \quad (14)$$

We discuss the global structure of the generalized Duffing's system by using this one-dimensional map.

If there is an m -periodic orbit of f then the dependence of m on B is obtained by applying a theory of intermittency. Approximating the discrete dynamic equation (14) by a differential equation

$$\frac{d\theta}{d\tau} \approx (2\nu+1)^{-1/2} (1/|B \cos 2\pi\theta|)^{\nu/(2\nu+1)} \quad (15)$$

and by integrating Eq. (15) one obtains, as the period,

$$\begin{aligned} T &\equiv \int_0^1 d\tau \\ &= B^{\nu/(2\nu+1)}(2\nu+1)^{1/2} \int_0^1 |\cos 2\pi\theta|^{\nu/(2\nu+1)} d\theta \\ &= C(\nu)B^{\nu/(2\nu+1)}, \end{aligned} \quad (16)$$

where $C(\nu)$ represents a constant independent of B . Since $T \propto m$ holds roughly in the m -periodic state, the scaling law is

$$B_m \propto m^{(2\nu+1)/\nu} \quad (17)$$

which explains excellently the experimentally observed results. In fact, the values of experimental results and theoretical results $\alpha_t \equiv (2\nu+1)/\nu$ are

$$\begin{aligned} \alpha &= 3.18, \quad \alpha_t = 3.0, \\ \alpha &= 2.57, \quad \alpha_t = 2.5, \\ \alpha &= 2.42, \quad \alpha_t = 2.33\dots, \end{aligned}$$

for $\nu = 1, 2$, and 3 , respectively.

Usually in the intermittency problem one considers a re-

ursion relation

$$x_{n+1} = x_n + ax_n^z + \epsilon,$$

where ϵ is a small parameter, for which it is well known that the scaling behavior for the m -periodic orbit in the limit of the small parameter approaching the critical value is $m \propto \epsilon^{-1+1/Z}$.¹⁷ In this paper, however, we have discussed an example of abnormal intermittency which can appear in a map of a circle onto itself or a forced nonlinear oscillator in the limit of the rotation number approaching zero. The map in this case can be expressed

$$\theta_{n+1} = f(\theta_n) = \theta_n + \epsilon g(\theta_n, \epsilon), \quad (18)$$

where ϵ is a control parameter and g is an arbitrary function. Considering a small deviation and expanding Eq. (18) by Taylor series around the fixed point of $f(\theta)$ and $\epsilon = 0$, one obtains a map f constituting the class of abnormal intermittency as $\epsilon \rightarrow 0$.¹⁰ Those maps belonging to the abnormal intermittency class have the scaling law for m -periodic orbit ($m = 2, 3, 4, \dots$) where $m \propto \epsilon^{-1}$ as $\epsilon \rightarrow 0$ and its scaling law is independent of $g(\theta, \epsilon)$.

¹M. J. Feigenbaum, *J. Stat. Phys.* **19**, 25 (1978); **21**, 669 (1979).

²Y. Pomeau and P. Manneville, *Commun. Math. Phys.* **74**, 189 (1980).

³D. Rand, S. Ostlund, J. Sethna, and E. D. Siggia, *Phys. Rev. Lett.* **49**, 132 (1982).

⁴L. Glass and R. Perez, *Phys. Rev. Lett.* **48**, 1772 (1982).

⁵K. Tomita and I. Tsuda, *Prog. Theor. Phys.* **62**, 185 (1980).

⁶K. Tomita and I. Tsuda, *Prog. Theor. Phys.* **64**, 1183 (1980).

⁷D. D'Humieres, M. R. Beasley, B. A. Huberman, and A. Libchaber, *Phys. Rev. A* **26**, 3483 (1982).

⁸N. F. Pedersen and A. Davidson, *Appl. Phys. Lett.* **39**, 830 (1981).

⁹J. E. Flaherty and F. C. Hoppenstead, *Stud. Appl. Math.* **58**, 5 (1978).

¹⁰K. Kaneko, *Prog. Theor. Phys.* **63**, 669 (1982).

¹¹M. Sano and Y. Sawada, *Phys. Lett. A* (in press).

¹²Y. Ueda, N. Akamatsu, and C. Hayashi, *Trans. I.E.C.E. Jpn.* **56A**, 218 (1979).

¹³Y. Ueda, in *Proceedings of the Engineering Foundation Conference on New Approaches to Nonlinear Problems in Dynamics*, edited by P. J. Holmes (SIAM, Philadelphia, 1979), p. 311.

¹⁴Y. Ueda, *Trans. I.E.C.E. Jpn.* **98A**, 167 (1979).

¹⁵H. Kawakami and J. Matsuo, *Trans. I.E.C.E. Jpn.* **64A**, 1018 (1981).

¹⁶S. J. Shenker, *Physica D* **5**, 405 (1982).

¹⁷For example, J. E. Hirsch, B. A. Huberman, and D. J. Scalapino, *Phys. Rev. A* **25**, 519 (1982).